

BENIGN OVERFITTING IN BINARY CLASSIFICATION OF GAUSSIAN MIXTURES

Ke Wang*

Christos Thrampoulidis†

*University of California, Santa Barbara, Department of Statistics and Applied Probability.

†University of California, Santa Barbara, Department of Electrical and Computer Engineering.

ABSTRACT

Deep neural networks generalize well despite being exceedingly overparametrized, but understanding the statistical principles behind this so called benign-overfitting phenomenon is not yet well understood. Recently there has been remarkable progress towards understanding benign-overfitting in simpler models, such as linear regression and, even more recently, linear classification. This paper studies benign-overfitting for data generated from a popular binary Gaussian mixtures model (GMM) and classifiers trained by support-vector machines (SVM). Our approach has two steps. First, we leverage an idea introduced in [MNS⁺20] to relate the SVM solution to the least-squares (LS) solution. Second, we derive novel non-asymptotic bounds on the classification error of LS solution. Combining the two gives sufficient conditions on the overparameterization ratio and the signal-to-noise ratio that lead to benign overfitting. We corroborate our theoretical findings with numerical simulations.

Index Terms— Overparameterization, SVM, Min-norm interpolation, Generalization error, Separable data

1. INTRODUCTION

Deep learning models are increasingly more complex with a huge number of parameters that far exceed the size of typical training data sets [MPCB14, PMR⁺17, GCB16]. As a consequence, after training, the models perfectly fit (or, so called interpolate) the data. Classical statistical wisdom would suggest that models that interpolate, overfit and as such they generalize poorly [HTF09]. But, the reality is very different in modern machine learning as such overparameterized learning architectures achieve state-of-the-art generalization performance despite interpolating the data. Understanding the principles behind this phenomenon – termed *benign overfitting* in [BLLT20] – is considered a central problem in modern learning theory and has attracted significant research attention over the past couple of years or so, e.g. [BHMM18, BHM18, MM19, LRZ19, LCM20, DKT19, BES⁺19, MNS⁺20].

By now there is rather long list of works explaining the phenomenon of benign overfitting in linear regression models including both asymptotic and non-asymptotic analyses [HMRT19, BHX19, MVSS20, TB20]. While certainly a sim-

plified model, studying linear regression is a natural first step towards understanding interpolating deep networks. A step further in this direction is the study of linear classification models, since arguably most success stories of deep learning apply to classification settings. Classification problems are not only more relevant, but also they are harder to analyze. One of the main reasons complicating the analysis is the fact that commonly used classifiers, such as support-vector machines (SVM), cannot be expressed in closed form – unlike least-squares (LS) solutions in linear regression.

Benign overfitting in binary linear classification has been recently investigated in e.g. [MRSY19, DKT19, KT20, MKLZ20, KA20, SAH20] in a linear asymptotic setting, where the size n of the training set and the size p of the parameter vector grow large at a fixed rate. These works overcome the aforementioned challenge by relying on powerful tools from modern high-dimensional statistics and yield asymptotic error predictions that are sharp [TOH15, TAH18]. However, the results only apply to the linear asymptotic regime. A different approach, resulting in more general non-asymptotic, albeit non-sharp, bounds was initiated in [MNS⁺20, CL20]. The key observation in [MNS⁺20, HMX20, KT20], that facilitates further analysis, is that in the overparameterized regime the SVM solution linearly interpolates the data. This allows the authors to establish a tight link between the (hard to directly analyze) SVM and the (amenable to analysis) LS solutions. In turn, this results in sufficient conditions on the data distribution leading to benign overfitting. The results in [MNS⁺20] hold for a ‘sign’ data model. While this paper was being prepared [HMX20] has extended the analysis to binary classification under generalized linear models.

In contrast to [MNS⁺20] that studied discriminative classification models, this paper undertakes a study of an alternative popular model. Specifically, we consider a Gaussian mixture model (GMM), which is a generative classification model. In GMM the feature vectors are distributed as Gaussians centered around the mean vector of the class to which they belong. In contrast, in the models studied in [MNS⁺20], the feature vectors are zero-mean Gaussians. This discrepancy significantly complicates the analysis and, as we show, it modifies the end results to account for the non-zero mean vectors.

We present two main results. First, we derive sufficient

conditions on the overparameterization ratio p/n and on the signal-to-noise ratio (SNR) so that the SVM solution linearly interpolates the data generated from the GMM. Second, we derive a novel non-asymptotic error bound on the LS solution for data generated from the GMM. Combining the two results, we identify sufficient conditions on p/n and on the SNR that lead to benign overfitting. Throughout, we present numerical results that corroborate our theoretical findings.

2. LEARNING MODEL

Notation. For a vectors $\mathbf{u} \in \mathbb{R}^p$ and $\mathbf{v} \in \mathbb{R}^p$, let $\|\mathbf{v}\|_2 = \sqrt{\sum_{i=1}^p v_i^2}$ and e_i denote the i -th standard basis vector. For a matrix \mathbf{M} , $\|\mathbf{M}\|_2$ denotes its operator norm. $[n]$ denotes the set $\{1, 2, \dots, n\}$. We also use standard "Big O" notations $\Theta(\cdot)$, $\omega(\cdot)$, e.g., see [CLRS09, Chapter 3]. Finally, we write $\mathcal{N}(\boldsymbol{\mu}, \boldsymbol{\Sigma})$ for the (multivariate) Gaussian distribution of mean $\boldsymbol{\mu}$ and covariance matrix $\boldsymbol{\Sigma}$, and, $Q(x) = \mathbb{P}(Z > x)$, $Z \sim \mathcal{N}(0, 1)$ for the Q-function of a standard normal.

2.1. Data model

Consider the following supervised binary classification problem under a *Gaussian mixtures model* (GMM). Let $\mathbf{x} \in \mathbb{R}^p$ denote the feature vector and $y \in \{-1, +1\}$ its class label. The class label y takes one of the values $\{\pm 1\}$ with probabilities $\pi_{\pm 1}$ such that $\pi_{+1} + \pi_{-1} = 1$. The class-conditional probability $p(\mathbf{x}|y)$ follows Gaussian distribution. Specifically, conditional on $y = \pm 1$, the feature vector \mathbf{x} is a Gaussian vector with mean vector $\pm \boldsymbol{\eta} \in \mathbb{R}^p$ and an invertible covariance matrix $\boldsymbol{\Sigma}$. Summarizing, the data pair (\mathbf{x}, y) is generated such that

$$y = \begin{cases} 1, & \text{w.p. } \pi_{+1} \\ -1, & \text{w.p. } 1 - \pi_{+1} \end{cases} \quad \text{and} \quad \mathbf{x}|y \sim \mathcal{N}(y\boldsymbol{\eta}, \boldsymbol{\Sigma}). \quad (1)$$

Consider training set $\{(\mathbf{x}_i, y_i)\}_{i=1}^n$ composed of n IID data pairs generated according to the GMM in (1). Let $\mathbf{X} = [\mathbf{x}_1, \mathbf{x}_2, \dots, \mathbf{x}_n]^T \in \mathbb{R}^{n \times p}$ denote the feature matrix and $\mathbf{y} = [y_1, \dots, y_n]^T$ denote the class-label vector. Following (1), the data matrix \mathbf{X} can be expressed as follows for a "noise matrix" $\mathbf{Q} \in \mathbb{R}^{n \times p}$ whose rows are independent $\mathcal{N}(\mathbf{0}, \boldsymbol{\Sigma})$ vectors,

$$\mathbf{X} = \mathbf{y}\boldsymbol{\eta}^T + \mathbf{Q}.$$

2.2. Training Algorithm

Given access to the training set, we train a linear classifier $\hat{\boldsymbol{\eta}}$ by minimizing the empirical risk $\hat{\mathcal{R}}_{\text{emp}}(\boldsymbol{\eta}) := \frac{1}{n} \sum_{i=1}^n \ell(y_i \boldsymbol{\eta}^T \mathbf{x}_i)$, where the loss function ℓ is chosen as: (i) Least-squares (LS): $\ell(t) = (1 - t)^2$, or, (ii) Logistic: $\ell(t) = \log(1 + e^{-t})$. Throughout, we focus on the *overparameterized* regime $p > n$. As is common, we run gradient descent (GD) on the empirical risk, until convergence. The

following results characterizing the *implicit bias* of GD for the square and logistic losses in the overparameterized regime are well-known. For one, when data can be linearly interpolated (i.e. $\exists \boldsymbol{\beta} \in \mathbb{R}^p$ such that $y_i = \mathbf{x}_i^T \boldsymbol{\beta}, \forall i \in [n]$), then GD on square loss converges to the solution of *min-norm interpolation* [HMRT19]:

$$\hat{\boldsymbol{\eta}}_{\text{LS}} = \arg \min_{\boldsymbol{\eta}} \|\boldsymbol{\eta}\|_2, \quad \text{subject to } y_i = \boldsymbol{\eta}^T \mathbf{x}_i, \forall i \in [n]. \quad (2)$$

Second, when data are linearly separable (i.e. $\exists \boldsymbol{\beta} \in \mathbb{R}^p$ such that $y_i(\mathbf{x}_i^T \boldsymbol{\beta}) \geq 1, \forall i \in [n]$), then (the normalized iterates of) GD on logistic loss converges to the solution of *hard-margin SVM* [SHN⁺18, JT19]:

$$\hat{\boldsymbol{\eta}}_{\text{SVM}} = \arg \min_{\boldsymbol{\eta}} \|\boldsymbol{\eta}\|_2, \quad \text{subject to } y_i \boldsymbol{\eta}^T \mathbf{x}_i \geq 1, \forall i \in [n]. \quad (3)$$

Now, it can be easily checked that when training data generated by the GMM and $p > n$, then the data can be linearly interpolated with high probability (whp.) (e.g., [KT20, HMX20]). Moreover, it is a simple exercise showing that this implies that the data are also linearly separable. Combining the above, in the overparameterized regime, whp., GD on data from the GMM converge to either (2) or (3) for a square and logistic loss, respectively.

Henceforth, we focus on the two classifiers in (3) and (2). In fact, in Section 3, we establish a link between the two.

2.3. Classification error

For a new sample (\mathbf{x}, y) , the classifier $\hat{\boldsymbol{\eta}}$ classifies \mathbf{x} as $\hat{y} = \text{sign}(\hat{\boldsymbol{\eta}}^T \mathbf{x})$. Then, the classification error is measured by the expected 0-1 loss risk

$$\mathcal{R}(\hat{\boldsymbol{\eta}}) = \mathbb{E}[\mathbb{I}(\hat{y} \neq y)] = \mathbb{P}(\hat{\boldsymbol{\eta}}^T (y\mathbf{x}) < 0), \quad (4)$$

where the expectation is over the distribution of (\mathbf{x}, y) generated as in (1). The following lemma gives an upper bound for $\mathcal{R}(\hat{\boldsymbol{\eta}})$.

Lemma 1. *The classification error of a classifier $\hat{\boldsymbol{\eta}}$ satisfies, $\mathcal{R}(\hat{\boldsymbol{\eta}}) = Q\left(\frac{\hat{\boldsymbol{\eta}}^T \boldsymbol{\eta}}{\sqrt{\hat{\boldsymbol{\eta}}^T \boldsymbol{\Sigma} \hat{\boldsymbol{\eta}}}}\right)$. In particular, if $\hat{\boldsymbol{\eta}}^T \boldsymbol{\eta} > 0$, then*

$$\mathcal{R}(\hat{\boldsymbol{\eta}}) \leq \exp\left(-\frac{(\hat{\boldsymbol{\eta}}^T \boldsymbol{\eta})^2}{2\hat{\boldsymbol{\eta}}^T \boldsymbol{\Sigma} \hat{\boldsymbol{\eta}}}\right).$$

Proof. For a new draw \mathbf{x}, y , using $\mathbf{x} = y\boldsymbol{\eta} + \boldsymbol{\Sigma}^{1/2} \mathbf{z}, \mathbf{z} \sim \mathcal{N}(\mathbf{0}, \mathbf{I})$ and symmetry of the Gaussian distribution, it can be easily checked that

$$\mathcal{R}(\hat{\boldsymbol{\eta}}) = \mathbb{P}(\hat{\boldsymbol{\eta}}^T (y\mathbf{x}) < -\hat{\boldsymbol{\eta}}^T \boldsymbol{\eta}) = \mathbb{P}(\boldsymbol{\Sigma}^{1/2} \hat{\boldsymbol{\eta}}^T \mathbf{z} > \hat{\boldsymbol{\eta}}^T \boldsymbol{\eta}).$$

Now, given $\hat{\boldsymbol{\eta}}, \boldsymbol{\Sigma}^{1/2} \hat{\boldsymbol{\eta}}^T (y\mathbf{z})$ is a zero-mean Gaussian random variable with variance $\hat{\boldsymbol{\eta}}^T \boldsymbol{\Sigma} \hat{\boldsymbol{\eta}}$. Thus, the advertised bounds follow directly: the first, by definition of the Q-function, and, the second, by the Chernoff bound for the Q-function [Wai19, Ch. 2]. \square

Thanks to the lemma above, our goal of upper bounding the classification error, reduces to that of lower bounding the ratio $\frac{(\hat{\eta}^T \eta)^2}{2\hat{\eta}^T \Sigma \hat{\eta}}$. We do this in Section 4 for the LS classifier. In large, this is possible thanks to the fact that the min-norm linear interpolator in (2) can be conveniently written in closed form $\hat{\eta}_{\text{LS}} = \mathbf{X}^T (\mathbf{X} \mathbf{X}^T)^{-1} \mathbf{y}$. In contrast, the SVM solution *cannot* be expressed in closed form. To go around this challenge, Section 3 establishes sufficient conditions under which the SVM-solution $\hat{\eta}_{\text{SVM}}$ linearly interpolates the data, thus, it coincides with the LS-solution.

Henceforth, we focus on the isotropic case $\Sigma = \mathbf{I}$. We leave the analysis of general covariance matrices to future work.

3. LINK BETWEEN SVM AND LINEAR-INTERPOLATION

This section establishes a link between the SVM solution in (3) and the LS solution in (2). Specifically, Theorem 1 below identifies sufficient conditions under which all training data points become support vectors, i.e., $\hat{\eta}_{\text{SVM}}$ linearly interpolates the data: $\mathbf{x}_i^T \hat{\eta}_{\text{SVM}} = y_i, \forall i \in [n]$.

Theorem 1. *Assume n training points following the GMM with $\Sigma = \mathbf{I}$. Let n be large enough. There exist positive constants $C_1, C_2 > 1$ such that, if the following conditions on the number of features p and the mean-vector η hold:*

$$p > 10n \log n + n - 1 \quad \text{and} \quad p > C_2 n \|\eta\|_2, \quad (5)$$

then, the SVM-solution $\hat{\eta}_{\text{SVM}}$ in (3) satisfies the linear interpolation constraint in (2) with probability at least $(1 - \frac{C_1}{n})$.

The theorem establishes two sufficient conditions for all training points to become support vectors. The first condition requires sufficient overparameterization: p be sufficiently large compared with n . The second one restricts the Euclidean norm of the mean vector to be no larger than a constant multiple of the overparameterization ratio p/n . Note from (1) that for $\Sigma = \mathbf{I}$, the squared-norm $\|\eta\|_2^2$ plays the role of SNR. Thus, the second condition requires that the SNR is not too high.

Now, we use numerical simulations to confirm that the conditions of the theorem, even though sufficient, capture the correct problem behavior. The two plots of Fig. 1(Left) shows the probability that all the training becoming support vectors as a function of n for different SNR values. The values shown are averages over 300 problem realizations. Here, we have set $p = 1500$ and vary n up to 125 to guarantee sufficient overparameterization according to the first condition in (5). In order to verify the second condition in (5), Fig. 1(Right) plots the same curves over a re-scaled axis $(n/p)\|\eta\|_2$ (as suggested by (5)). Note that the three curves corresponding to different SNR values overlap in this new scaling, which agrees with the prediction of Theorem 1.

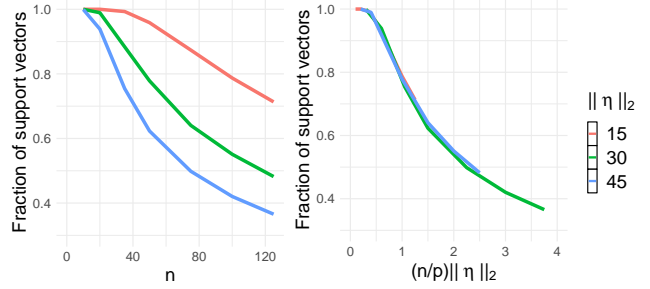


Fig. 1. Proportion of support vectors for various values of SNR = $\|\eta\|_2^2$. Here, $p = 1500$ and values shown are averages over 300 realizations. Note that the three curves overlap when plotted versus $(n/p)\|\eta\|_2$ as predicted by Theorem 1.

Theorem 1 is useful for our purpose of studying the classification error of $\hat{\eta}_{\text{SVM}}$ since: *if (5) holds, then $\hat{\eta}_{\text{SVM}} = \hat{\eta}_{\text{LS}} = \mathbf{X}^T (\mathbf{X} \mathbf{X}^T)^{-1} \mathbf{y}$.* Thus, under these conditions we can analyze the classification error (3), by studying the simpler LS solution in (2). This observation was recently first exploited in [MNS⁺20], but for a rather different data model. To see why the above statement is true, note that when (5) holds, then $\hat{\eta}_{\text{SVM}}$ satisfies the linear interpolation constraints; thus, it is feasible in (2). Consequently, $\hat{\eta}_{\text{SVM}}$ is in fact optimal in (2). To see the latter, assume for the sake of contradiction that $\|\hat{\eta}_{\text{LS}}\|_2 < \|\hat{\eta}_{\text{SVM}}\|_2$. But, for all $i \in [n]$, $y_i(\hat{\eta}_{\text{LS}}^T \mathbf{x}_i) = y_i^2 \geq 1$; thus, $\hat{\eta}_{\text{LS}}$ is feasible in (3), which contradicts our assumption.

As mentioned, [MNS⁺20] established similar conditions to Theorem 1, but for a ‘Signed’ model, where $\mathbf{x}_i \sim \mathcal{N}(\mathbf{0}, \Sigma)$ and $y_i = \text{sign}(\mathbf{x}_i^T \eta)$. Interestingly, for the isotropic case $\Sigma = \mathbf{I}$, they obtained a sufficient condition that is identical to the first condition in (5). The second condition in (5) appears to be tailored to the GMM. Intuitively, this is explained since in the ‘Signed’ model the data are insensitive to the value of the SNR $\|\eta\|_2^2$; what matters is only the direction of η . In contrast, both the direction and the scaling of the mean vector η are important in the GMM as apparent from (1). Our analysis leading to Theorem 1 captures this in a concrete way.

4. CLASSIFICATION ERROR OF MIN-NORM LINEAR INTERPOLATION

This section includes our second main result: an upper bound on the classification error of the min-norm LS solution $\hat{\eta}_{\text{LS}}$ in the isotropic setting.

To begin with, recall from Lemma 1 that $\hat{\eta}_{\text{LS}}^T \eta > 0$ is needed to ensure that $\mathcal{R}(\hat{\eta}_{\text{LS}}) < 1/2$. The next lemma shows that this favorable event occurs with high probability provided sufficiently large overparameterization and SNR.

Lemma 2. *Fix $\delta \in (0, 1)$ and suppose n is large enough such that $n > c \log(1/\delta)$ for some $c > 1$. Then, there exist*

constants $C, b > 1$ such that with probability at least $1 - \delta$, $\hat{\eta}_{\text{LS}}^T \eta \geq 0$ provided that

$$p > b \cdot n \quad \text{and} \quad \left(1 - \frac{n}{p}\right) \|\eta\|_2 > C. \quad (6)$$

Now we are ready to state the main result.

Theorem 2. Fix $\delta \in (0, 1)$ and suppose n is large enough such that $n > c \log(1/\delta)$ for some $c > 1$. Further assume that (6) holds for constants $b, C > 1$. Then, there exists constants $C_1, C_2 > 1$ such that with probability at least $1 - \delta$, the expected 0-1 loss of the least squares min-norm solution $\hat{\eta}_{\text{LS}}$ satisfies:

$$\mathcal{R}(\hat{\eta}_{\text{LS}}) \leq \exp \left(-\|\eta\|_2^2 \frac{\left(1 - \frac{n}{p}\right) \|\eta\|_2 - C_1}{C_2 \left(\frac{p}{n} + \|\eta\|_2^2\right)} \right). \quad (7)$$

As expected, the bound on $\mathcal{R}(\hat{\eta}_{\text{LS}})$ depends on the over-parameterization ratio p/n and the SNR $\|\eta\|_2^2$. To clarify the dependence, it is instructive to consider separately the following two regimes.

- High-SNR regime $\|\eta\|_2^2 > \frac{p}{n}$.
- Low-SNR regime: $\|\eta\|_2^2 \leq \frac{p}{n}$.

The following is an immediate corollary of Theorem 2.

Corollary 2.1. Let the same assumptions of Theorem 2 hold. Then, there exists constants $C_1 > 1, C_2 > 0$ such that with probability at least $1 - \delta$, in the high-SNR regime:

$$\mathcal{R}(\hat{\eta}_{\text{LS}}) \leq \exp \left(-C_2 \cdot \|\eta\|_2^2 \cdot \left(\left(1 - \frac{n}{p}\right) - C_1 \frac{1}{\|\eta\|_2} \right)^2 \right), \quad (8)$$

and, in the low-SNR regime:

$$\mathcal{R}(\hat{\eta}_{\text{LS}}) \leq \exp \left(-C_2 \cdot \|\eta\|_2^4 \frac{\left(\left(1 - \frac{n}{p}\right) - C_1 \frac{1}{\|\eta\|_2} \right)^2}{p/n} \right). \quad (9)$$

We use numerical simulations to validate the above bounds. In Fig. 2(Top) we fix $n = 100$ and plot the test classification error (in log-scale) as a function of p for four different SNR values 3, 5, 8 and 10. The values shown are averages over 300 independent monte-carlo realizations. Observe that $-\log \mathcal{R}(\hat{\eta}_{\text{LS}})$ initially increases until it reaches its maximum at some value of $p > n$ and then decreases as p gets even larger. This “increasing/decreasing” pattern is explained by the transition from the high-SNR regime to the low-SNR regime as per Corollary 2.1. On the one hand, the negative of the exponent of the high-SNR bound (8) is increasing with p for $\|\eta\|_2^2$. On the other hand, as p increases, and we move in the low-SNR regime, the negative of the exponent in (9) decreases with p when p is large enough. Additionally, in Figs. 2(Bottom-Left) and 2(Bottom-Right), we plot re-normalized values $-\log \mathcal{R}(\hat{\eta}_{\text{LS}})/\|\eta\|_2^2$ and $-\log \mathcal{R}(\hat{\eta}_{\text{LS}})/\|\eta\|_2^4$. Notice that after appropriately normalizing with the SNR, the curves become almost parallel to each other and almost overlap for large values of $\|\eta\|_2^2$, which agrees with both (9) and (8).

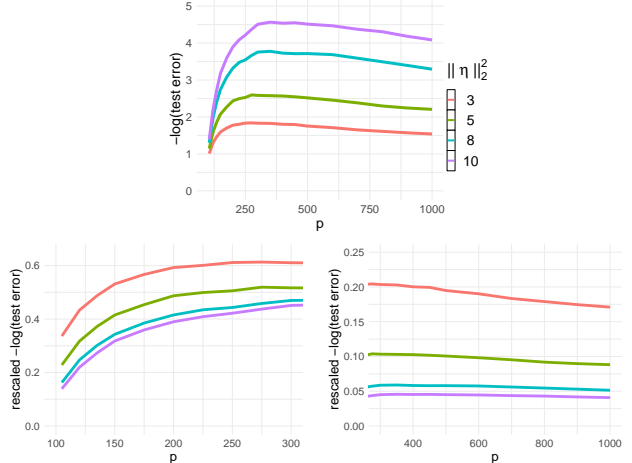


Fig. 2. The top plot shows $-\log(\text{test classification error})$ with $\|\eta\|_2^2 = 3, 5, 8, 10$. The bottom figures show the $-\log(\text{test error})/\|\eta\|_2^2$ for small p and $-\log(\text{test error})/\|\eta\|_2^4$ for large p respectively. The bottom plots are consistent with results (9) and (8) respectively. The negative log classification error curves become almost parallel after making the adjustment based on Corollary 2.1

5. BENIGN OVERFITTING

Now that we have captured the classification error of the min-norm LS solution $\hat{\eta}_{\text{LS}}$ in Theorem 2, and, we have shown when $\hat{\eta}_{\text{SVM}} = \hat{\eta}_{\text{LS}}$ in Theorem 1, we are ready to establish sufficient conditions under which the classification error of hard-margin SVM (eqv. gradient descent on logistic loss) vanishes as p gets larger.

Corollary 2.2. For sufficiently large n and large positive constant $C_1 > 1$, $\hat{\eta}_{\text{SVM}}$ linearly interpolates the data and the classification error $\mathcal{R}(\hat{\eta}_{\text{SVM}})$ approaches zero as $p \rightarrow \infty$ with probability at least $(1 - \frac{C_1}{n})$ if the following conditions on the number of features p and mean-vector η hold: $p > 10n \log n + n - 1$ and $n\|\eta\|_2 = \Theta(p^\tau)$ for some $\tau \in (\frac{1}{4}, 1)$.

Proof. First, we use Corollary 2.1 to derive conditions that ensure good generalization. Notice that $n\|\eta\|_2 = \omega(p^{\frac{1}{2}})$ suffices to satisfy the high-SNR regime assumption. But, then the classification error goes to zero with growing p , since from (8) $\cdot \|\eta\|_2^2 \cdot \left(\left(1 - \frac{n}{p}\right) - C_1 \frac{1}{\|\eta\|_2} \right)^2 = \omega(p)$. Similarly, it can be checked from (9) that $n\|\eta\|_2 = \omega(p^{\frac{1}{4}})$ suffices to make the classification error go to zero as $p \rightarrow \infty$ in the low-SNR regime. Combining the above, it suffices for benign overfitting that $n\|\eta\|_2 = \omega(p^{\frac{1}{4}})$. Next, we combine this with (5), which guarantees that the above conclusion based on Corollary 2.1 applies to the SVM solution. Specifically, we need $p > 10n \log n + n - 1$ and $n\|\eta\|_2 = O(p)$. This completes the proof. \square

Next, we present numerical illustrations validating the

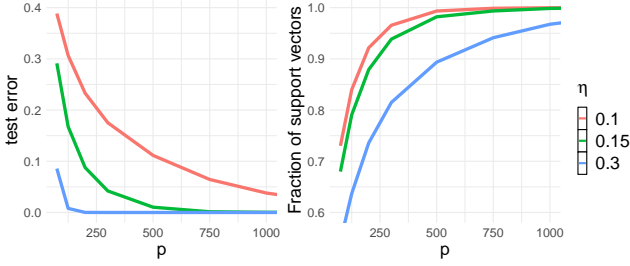


Fig. 3. The left plot shows the test classification error under the isotropic ensemble with $n = 50$ and mean vector η with entries $\eta_1 = \dots = \eta_p = \eta$. The test error vanishes with $p \rightarrow \infty$. The right plot illustrates the proportion of support vectors in the same setting. All the data points are support vectors for sufficiently large p . These confirm the predictions of Corollary 2.2 on benign overfitting.

predictions of the corollary. We let $\eta_1 = \dots = \eta_p = \eta$ with $\eta = 0.1, 0.15$, or 0.3 . Thus, $\|\eta\|_2 = \eta\sqrt{p}$. We also fix $n = 50$. These guarantee that $n\|\eta\|_2 = \Theta(p^{1/2})$ satisfying the second condition of the corollary. In Fig. 3(Left), we plot the test classification error as a function of p . The values shown are averages over 300 realizations. We verify that as p increases, the test classification error decreases towards zero. Similarly, Fig. 3(Right) reaffirms that the all the data points become support vectors for sufficiently large p (cf. Theorem 1).

Finally, we comment on how our result compares to [CL20]. Using different analysis, in their recent work [CL20] proved that $\|\eta\|_2^4 = \omega(p)$ suffices for benign overfitting, i.e., for making the classification error vanish as $p \rightarrow \infty$. In comparison, (8) shows that we only need $\|\eta\|_2^4 = \omega(p/n)$. to achieve zero classification error as $p \rightarrow \infty$, which relaxes the condition of [CL20].

6. PROOFS OUTLINE

The proofs of Theorems 1 and 2 are related. Hence we discuss them here together. The complete proofs of the theorems are given in the appendix.

Reduction to quadratic terms of the Gram-matrix. First, we show that the proofs of both of the theorems reduce to establishing lower/upper bounds on quadratic forms of the Gram matrix $(\mathbf{X}\mathbf{X}^T)^{-1}$. We start with Theorem 1. As in the proof of [MNS⁺20, Theorem 1], it suffices to derive conditions under which the following complementary slackness condition of (3) is satisfied with high probability:

$$y_i e_i^T (\mathbf{X}\mathbf{X}^T)^{-1} \mathbf{y} > 0, \text{ for } i \in [n]. \quad (10)$$

Note that (10) is a quadratic form involving $(\mathbf{X}\mathbf{X}^T)^{-1}$. Next, to prove Theorem 2, it suffices from Lemma 1 that we lower bound the ratio $\frac{(\hat{\eta}_{\text{LS}}^T \eta)^2}{\hat{\eta}_{\text{LS}}^T \hat{\eta}_{\text{LS}}} = \frac{(y^T (\mathbf{X}\mathbf{X}^T)^{-1} \mathbf{X} \eta)^2}{y^T (\mathbf{X}\mathbf{X}^T)^{-1} y}$. Our key

technical contribution is deriving upper and lower bounds for $y^T (\mathbf{X}\mathbf{X}^T)^{-1} y$. Similar to the problem above in the proof of Theorem 1, note that this is a quadratic form involving $(\mathbf{X}\mathbf{X}^T)^{-1}$.

Challenge. Bounding quadratic forms involving the Gram matrix $(\mathbf{X}\mathbf{X}^T)^{-1}$ is challenging for the GMM. The reason is that $\mathbf{X}\mathbf{X}^T = (y\eta^T + \mathbf{Q})(y\eta^T + \mathbf{Q})^T$. Thus the Gram matrix “includes” y . In particular this is different to previous works [MNS⁺20, BLLT20], since in their setting $\mathbf{X}\mathbf{X}^T = \mathbf{Q}\mathbf{Q}^T$.

Our approach. For concreteness, consider the problem of bounding the quadratic form $y^T (\mathbf{X}\mathbf{X}^T)^{-1} y$ as needed for Theorem 2. A possible approach is to start from bounds on the eigenvalues of $\mathbf{X}\mathbf{X}^T$ and then obtain bounds for the eigenvalues of its inverse. In this spirit, [BLLT20, MNS⁺20], who studied related problems, provide bounds for the eigenvalues of $\mathbf{Q}\mathbf{Q}^T$, which they then use to bound quadratic forms involving $(\mathbf{Q}\mathbf{Q}^T)^{-1}$. Our task is more challenging, because \mathbf{X} includes the addition term $y\eta^T$. In particular, since \mathbf{X} depends on y , attempting to bound $y^T (\mathbf{X}\mathbf{X}^T)^{-1} y$ using the eigenvalue approach as suggested above is suboptimal since it ignores that dependence. Instead, we consider $y^T (\mathbf{X}\mathbf{X}^T)^{-1} y$ as a whole and work on the inverse directly. Specifically our idea is to decompose the Gram matrix $\mathbf{X}\mathbf{X}^T$ as follows:

$$\mathbf{X}\mathbf{X}^T = \mathbf{Q}\mathbf{Q}^T + [\|\eta\|_2 y, \mathbf{Q}\eta, y] [\|\eta\|_2 y, \mathbf{Q}\eta, y]^T.$$

Then, we apply the Woodbury matrix inverse identity to the matrix form above. After some algebra steps we find that

$$y^T (\mathbf{X}\mathbf{X}^T)^{-1} y = s / (s(\|\eta\|_2^2 - t) + (h + 1)^2) \quad (11)$$

where $\mathbf{U} := \mathbf{Q}\mathbf{Q}^T$, $\mathbf{d} := \mathbf{Q}\eta$, $s := y^T \mathbf{U}^{-1} y$, $t := \mathbf{d}^T \mathbf{U}^{-1} \mathbf{d}$ and $h := y^T \mathbf{U}^{-1} \mathbf{d}$. The remaining of the proof involves lower and upper bounding the terms s , t and h . Note that this is a simpler task as it involves bounding eigenvalues of the inverse of $\mathbf{Q}\mathbf{Q}^T$. We accomplish this leveraging the techniques of [BLLT20].

7. FUTURE WORK

We established a connection between the SVM and the LS solutions in the overparameterized regime for a GMM with isotropic features. We also proved a non-asymptotic bound for the test classification error, which we used to study benign overfitting. We believe that our techniques extend to the anisotropic case $\Sigma \neq \mathbf{I}$ and we plan to study this next. Other extensions include investigating the effect of label noise and misspecified models in our results. Possible extensions to more complex nonlinear settings are naturally very important.

Acknowledgments

C. Thrampoulidis is partially supported by the NSF under Grant Number CCF-2009030.

8. REFERENCES

- [BES⁺19] Jimmy Ba, Murat Erdogdu, Taiji Suzuki, Denny Wu, and Tianzong Zhang. Generalization of two-layer neural networks: An asymptotic viewpoint. In *International Conference on Learning Representations*, 2019.
- [BHM18] Mikhail Belkin, Daniel J Hsu, and Partha Mitra. Overfitting or perfect fitting? risk bounds for classification and regression rules that interpolate. In *Advances in neural information processing systems*, pages 2300–2311, 2018.
- [BHMM18] Mikhail Belkin, Daniel Hsu, Siyuan Ma, and Soumik Mandal. Reconciling modern machine learning and the bias-variance trade-off. *stat*, 1050:28, 2018.
- [BHX19] Mikhail Belkin, Daniel Hsu, and Ji Xu. Two models of double descent for weak features. *arXiv preprint arXiv:1903.07571*, 2019.
- [BLLT20] Peter L Bartlett, Philip M Long, Gábor Lugosi, and Alexander Tsigler. Benign overfitting in linear regression. *Proceedings of the National Academy of Sciences*, 2020.
- [CL20] Niladri S Chatterji and Philip M Long. Finite-sample analysis of interpolating linear classifiers in the overparameterized regime. *arXiv preprint arXiv:2004.12019*, 2020.
- [CLRS09] Thomas H Cormen, Charles E Leiserson, Ronald L Rivest, and Clifford Stein. *Introduction to algorithms*. MIT press, 2009.
- [DKT19] Zeyu Deng, Abla Kammoun, and Christos Thrampoulidis. A model of double descent for high-dimensional binary linear classification. *arXiv preprint arXiv:1911.05822*, 2019.
- [GBCB16] Ian Goodfellow, Yoshua Bengio, Aaron Courville, and Yoshua Bengio. *Deep learning*, volume 1. MIT press Cambridge, 2016.
- [HJ12] Roger A Horn and Charles R Johnson. *Matrix analysis*. Cambridge university press, 2012.
- [HMRT19] Trevor Hastie, Andrea Montanari, Saharon Rosset, and Ryan J Tibshirani. Surprises in high-dimensional ridgeless least squares interpolation. *arXiv preprint arXiv:1903.08560*, 2019.
- [HMX20] Daniel Hsu, Vidya Muthukumar, and Ji Xu. On the proliferation of support vectors in high dimensions. *arXiv preprint arXiv:2009.10670*, 2020.
- [HTF09] Trevor Hastie, Robert Tibshirani, and Jerome Friedman. *The elements of statistical learning: data mining, inference, and prediction*. Springer Science & Business Media, 2009.
- [JT19] Ziwei Ji and Matus Telgarsky. The implicit bias of gradient descent on nonseparable data. In *Conference on Learning Theory*, pages 1772–1798, 2019.
- [KA20] Abla Kammoun and Mohamed-Slim Alouini. On the precise error analysis of support vector machines. *arXiv preprint arXiv:2003.12972*, 2020.
- [KT20] Ganesh Kini and Christos Thrampoulidis. Analytic study of double descent in binary classification: The impact of loss. *arXiv preprint arXiv:2001.11572*, 2020.
- [LCM20] Zhenyu Liao, Romain Couillet, and Michael W Mahoney. A random matrix analysis of random fourier features: beyond the gaussian kernel, a precise phase transition, and the corresponding double descent. *arXiv preprint arXiv:2006.05013*, 2020.
- [LRZ19] Tengyuan Liang, Alexander Rakhlin, and Xiyu Zhai. On the risk of minimum-norm interpolants and restricted lower isometry of kernels. *arXiv preprint arXiv:1908.10292*, 2019.
- [MKLZ20] Francesca Mignacco, Florent Krzakala, Yue M Lu, and Lenka Zdeborová. The role of regularization in classification of high-dimensional noisy gaussian mixture. *arXiv preprint arXiv:2002.11544*, 2020.
- [MM19] Song Mei and Andrea Montanari. The generalization error of random features regression: Precise asymptotics and double descent curve. *arXiv preprint arXiv:1908.05355*, 2019.

[MNS⁺20] Vidya Muthukumar, Adhyyan Narang, Vignesh Subramanian, Mikhail Belkin, Daniel Hsu, and Anant Sahai. Classification vs regression in overparameterized regimes: Does the loss function matter? *arXiv preprint arXiv:2005.08054*, 2020.

[MPCB14] Guido F Montufar, Razvan Pascanu, Kyunghyun Cho, and Yoshua Bengio. On the number of linear regions of deep neural networks. In *Advances in neural information processing systems*, pages 2924–2932, 2014.

[MRSY19] Andrea Montanari, Feng Ruan, Youngtak Sohn, and Jun Yan. The generalization error of max-margin linear classifiers: High-dimensional asymptotics in the overparametrized regime. *arXiv preprint arXiv:1911.01544*, 2019.

[MVSS20] Vidya Muthukumar, Kailas Vodrahalli, Vignesh Subramanian, and Anant Sahai. Harmless interpolation of noisy data in regression. *IEEE Journal on Selected Areas in Information Theory*, 2020.

[PMR⁺17] Tomaso Poggio, Hrushikesh Mhaskar, Lorenzo Rosasco, Brando Miranda, and Qianli Liao. Why and when can deep-but not shallow-networks avoid the curse of dimensionality: a review. *International Journal of Automation and Computing*, 14(5):503–519, 2017.

[SAH20] Fariborz Salehi, Ehsan Abbasi, and Babak Hassibi. The performance analysis of generalized margin maximizer (gmm) on separable data. *arXiv preprint arXiv:2010.15379*, 2020.

[SHN⁺18] Daniel Soudry, Elad Hoffer, Mor Shpigel Nacson, Suriya Gunasekar, and Nathan Srebro. The implicit bias of gradient descent on separable data. *The Journal of Machine Learning Research*, 19(1):2822–2878, 2018.

[TAH18] Christos Thrampoulidis, Ehsan Abbasi, and Babak Hassibi. Precise error analysis of regularized m -estimators in high dimensions. *IEEE Transactions on Information Theory*, 64(8):5592–5628, 2018.

[TB20] Alexander Tsigler and Peter L Bartlett. Benign overfitting in ridge regression. *arXiv preprint arXiv:2009.14286*, 2020.

[TOH15] Christos Thrampoulidis, Samet Oymak, and Babak Hassibi. Regularized linear regression: A precise analysis of the estimation error. *Proceedings of Machine Learning Research*, 40:1683–1709, 2015.

[Ver18] Roman Vershynin. *High-dimensional probability: An introduction with applications in data science*, volume 47. Cambridge university press, 2018.

[Wai19] Martin J Wainwright. *High-dimensional statistics: A non-asymptotic viewpoint*, volume 48. Cambridge University Press, 2019.

A. KEY TECHNICAL LEMMAS

Let $\mathbf{U} := \mathbf{Q}\mathbf{Q}^T$ and $\mathbf{d} := \mathbf{Q}\boldsymbol{\eta}$. As we mentioned in Section 6, one main challenge is to bound quadratic forms involving the Gram matrix $(\mathbf{X}\mathbf{X}^T)^{-1}$. Specifically, we need to bound $\mathbf{y}^T(\mathbf{X}\mathbf{X}^T)^{-1}\mathbf{e}_i$, $\mathbf{y}^T(\mathbf{X}\mathbf{X}^T)^{-1}\mathbf{y}$ and $\mathbf{y}^T(\mathbf{X}\mathbf{X}^T)^{-1}\mathbf{d}$. Consider the following quadratic forms involving the inverse Gram matrix \mathbf{U}^{-1} :

$$\begin{aligned} s &= \mathbf{y}^T \mathbf{U}^{-1} \mathbf{y}, \\ t &= \mathbf{d}^T \mathbf{U}^{-1} \mathbf{d}, \\ h &= \mathbf{y}^T \mathbf{U}^{-1} \mathbf{d}, \\ g_i &= \mathbf{y}^T \mathbf{U}^{-1} \mathbf{e}_i, \\ f_i &= \mathbf{d}^T \mathbf{U}^{-1} \mathbf{e}_i. \end{aligned}$$

The following lemma expresses $\mathbf{y}^T(\mathbf{X}\mathbf{X}^T)^{-1}$ in terms of those quadratic forms.

Lemma 3. Define $D := s(\|\boldsymbol{\eta}\|_2^2 - t) + (h + 1)^2$, then

$$\mathbf{y}^T(\mathbf{X}\mathbf{X}^T)^{-1} = \mathbf{y}^T \mathbf{U}^{-1} - \frac{1}{D} \left[\|\boldsymbol{\eta}\|_2 s, h^2 + h - st, s \right] \begin{bmatrix} \|\boldsymbol{\eta}\|_2 \mathbf{y}^T \\ \mathbf{y}^T \\ \mathbf{d}^T \end{bmatrix} \mathbf{U}^{-1}. \quad (12)$$

The following lemma derives the upper/lower bounds for those quadratic forms involving the inverse Gram matrix \mathbf{U}^{-1} .

Lemma 4. *Fix $\delta \in (0, 1)$ and suppose n is large enough such that $n > c \log(1/\delta)$ for some $c > 1$. Further assume that $p > bn$ holds for some constant $b > 1$. Then, there exists constants $C_1, C_2, C_3 > 1$, $C_4, C_5 > 0$ such that with probability at least $1 - \delta$, the following results hold:*

$$\begin{aligned} \frac{n}{C_1 p} \leq s &\leq C_1 \frac{n}{p}, \\ C_4 \frac{n}{p} \|\boldsymbol{\eta}\|_2^2 \leq t &\leq C_5 \frac{n}{p} \|\boldsymbol{\eta}\|_2^2, \\ -C_2 \frac{n}{p} \|\boldsymbol{\eta}\|_2 &\leq h \leq C_2 \frac{n}{p} \|\boldsymbol{\eta}\|_2, \\ -C_3 \frac{\sqrt{n}}{p} \|\boldsymbol{\eta}\|_2 &\leq f_i \leq C_3 \frac{\sqrt{n}}{p} \|\boldsymbol{\eta}\|_2, \text{ for } i \in [n]. \end{aligned}$$

The proof of Lemma 3 and 4 are given in Section D. We will also need the following lemma adapted from [MNS⁺20, Lemma 2].

Lemma 5. *Let $d'(n) := (p - n + 1)$. With probability at least $(1 - \frac{2}{n^2})$,*

$$y_i g_i = y_i (\mathbf{e}_i^T \mathbf{U}^{-1} \mathbf{y}) \geq C \frac{2\sqrt{n}d'(n) - 2n\sqrt{4\log(n)d'(n)} - 4n\log(n)}{(d'(n) + \sqrt{4\log(n)d'(n)})(d'(n) - \sqrt{4\log(n)d'(n)})}, \text{ for } i \in [n].$$

B. PROOF OF THEOREM 1

Now we are ready to prove Theorem 1. Define $\gamma^* := (\mathbf{X}\mathbf{X}^T)^{-1} \mathbf{y}$. Using duality (see [MNS⁺20, Appendix C.1]), all the constraints in (3) hold with equality provided that

$$y_i \gamma_i^* > 0, \text{ for } i = 1, \dots, n. \quad (13)$$

Hence it suffices to derive conditions under which (13) holds with high probability. Note that

$$\gamma_i^* = \mathbf{y}^T (\mathbf{X}\mathbf{X}^T)^{-1} \mathbf{e}_i, \text{ for } i = 1, \dots, n.$$

Using (12) and some algebra steps, it can be checked that:

$$\mathbf{y}^T (\mathbf{X}\mathbf{X}^T)^{-1} \mathbf{e}_i = g_i - \frac{1}{D} \left[\|\boldsymbol{\eta}\|_2 s, h^2 + h - st, s \right] \begin{bmatrix} \|\boldsymbol{\eta}\|_2 g_i \\ g_i \\ f_i \end{bmatrix} \quad (14)$$

$$= \frac{g_i + hg_i - sf_i}{s(\|\boldsymbol{\eta}\|_2^2 - t) + (h + 1)^2}. \quad (15)$$

Here, s, h, t, g_i and f_i are defined in Section A. The denominator of (15) is positive for large n and p , thus to make $\gamma_i > 0$, we only need to study the numerator:

$$y_i(g_i + hg_i - sf) = (1 + \mathbf{y}^T \mathbf{U}^{-1} \mathbf{d}) y_i (\mathbf{e}_i^T \mathbf{U}^{-1} \mathbf{y}) - y_i (\mathbf{e}_i^T \mathbf{U}^{-1} \mathbf{d}) \mathbf{y}^T \mathbf{U}^{-1} \mathbf{y}.$$

First, consider the term $y_i (\mathbf{e}_i^T \mathbf{U}^{-1} \mathbf{y})$. By Lemma 5, if $d'(n) = p - n + 1 > 9n \log(n)$, then,

$$y_i g_i = y_i (\mathbf{e}_i^T \mathbf{U}^{-1} \mathbf{y}) > \frac{2\sqrt{n}d'(n) - \frac{4}{3}\sqrt{n}d'(n) - \frac{4}{9}d'(n)}{2d'(n)^2} \quad (16)$$

$$> \frac{1}{10} \frac{\sqrt{n}}{p}. \quad (17)$$

Second, by Lemma 4 and (17) we find that

$$\begin{aligned}
y_i(g_i + cg_i - sf) &= (1 + h)y_i g_i - y_i s f \\
&\geq (1 - |h|) \frac{\sqrt{n}}{10p} - |f|s \\
&\geq \frac{\sqrt{np} - 10C \sqrt{\frac{n}{p}} n \|\boldsymbol{\eta}\|_2}{10p^{1.5}}.
\end{aligned}$$

To make the expression above positive, it suffices to have

$$p > 10Cn\|\boldsymbol{\eta}\|_2.$$

The result above holds for every $\gamma_i^*, i \in [n]$ with probability $1 - \frac{C}{n^2}$ each (by Lemma 5). Applying union bound over all n training data points, we conclude that $y_i \gamma_i^* > 0$ for all i with probability at least $1 - \frac{C_1}{n}$. This completes the proof.

C. PROOF OF THEOREM 2

From Section 6, we need to lower bound the ratio

$$\frac{(\mathbf{y}^T(\mathbf{X}\mathbf{X}^T)^{-1}\mathbf{X}\boldsymbol{\eta})^2}{\mathbf{y}^T(\mathbf{X}\mathbf{X}^T)^{-1}\mathbf{y}}. \quad (18)$$

Here we will lower bound $\mathbf{y}^T(\mathbf{X}\mathbf{X}^T)^{-1}\mathbf{X}\boldsymbol{\eta}$ and upper bound $\mathbf{y}^T(\mathbf{X}\mathbf{X}^T)^{-1}\mathbf{y}$. By Lemma 1, we know that the bound is not useful if $\mathbf{y}^T(\mathbf{X}\mathbf{X}^T)^{-1}\mathbf{X}\boldsymbol{\eta} < 0$, hence we need the conditions that ensure $\mathbf{y}^T(\mathbf{X}\mathbf{X}^T)^{-1}\mathbf{X}\boldsymbol{\eta} \geq 0$ with high probability. Using (12) and some algebra steps, it can be checked that:

$$\begin{aligned}
\mathbf{y}^T(\mathbf{X}\mathbf{X}^T)^{-1}\mathbf{y} &= s - \frac{\|\boldsymbol{\eta}\|_2^2 s^2 + sh^2 + 2sh - s^2 t}{s(\|\boldsymbol{\eta}\|_2^2 - t) + (h + 1)^2} \\
&= \frac{s}{s(\|\boldsymbol{\eta}\|_2^2 - t) + (h + 1)^2}.
\end{aligned}$$

Similarly,

$$\begin{aligned}
\mathbf{y}^T(\mathbf{X}\mathbf{X}^T)^{-1}\mathbf{X}\boldsymbol{\eta} &= \|\boldsymbol{\eta}\|_2^2 \mathbf{y}^T(\mathbf{X}\mathbf{X}^T)^{-1}\mathbf{y} + \mathbf{y}^T(\mathbf{X}\mathbf{X}^T)^{-1}\mathbf{Q}\boldsymbol{\eta} \\
&= \|\boldsymbol{\eta}\|_2^2 \mathbf{y}^T(\mathbf{X}\mathbf{X}^T)^{-1}\mathbf{y} + \mathbf{y}^T(\mathbf{X}\mathbf{X}^T)^{-1}\mathbf{d} \\
&= \frac{-st + h^2 + h}{s(\|\boldsymbol{\eta}\|_2^2 - t) + (h + 1)^2}.
\end{aligned}$$

Combining the above gives

$$\frac{(\mathbf{y}^T(\mathbf{X}\mathbf{X}^T)^{-1}\mathbf{X}\boldsymbol{\eta})^2}{\mathbf{y}^T(\mathbf{X}\mathbf{X}^T)^{-1}\mathbf{y}} = \frac{\left(s(\|\boldsymbol{\eta}\|_2^2 - t) + h^2 + h\right)^2}{s\left(s(\|\boldsymbol{\eta}\|_2^2 - t) + (h + 1)^2\right)}. \quad (19)$$

The numerator needs to be lower bounded and Lemma 4 gives with probability at least $1 - \delta$,

$$s(\|\boldsymbol{\eta}\|_2^2 - t) + h^2 + h \geq s(\|\boldsymbol{\eta}\|_2^2 - t) + h \quad (20)$$

$$\geq \frac{n}{C_1 p} \left(1 - \frac{n}{p}\right) \|\boldsymbol{\eta}\|_2^2 - C_2 \frac{n}{p} \|\boldsymbol{\eta}\|_2 \quad (21)$$

$$\geq \frac{n}{C_1 p} \left(\left(1 - \frac{n}{p}\right) \|\boldsymbol{\eta}\|_2^2 - C_3 \|\boldsymbol{\eta}\|_2\right). \quad (22)$$

Similarly, the denominator is upper bounded by:

$$\begin{aligned}
s(s(\|\boldsymbol{\eta}\|_2^2 - t) + (h+1)^2) &\leq s\left(s\|\boldsymbol{\eta}\|_2^2 + (1+|h|)^2\right) \\
&\leq C_1 \frac{n}{p} \left(C_1 \frac{n}{p} \|\boldsymbol{\eta}\|_2^2 + (1+C_2 \frac{n}{p} \|\boldsymbol{\eta}\|_2)^2\right) \\
&\leq C_1 \frac{n}{p} \left(C_3 \frac{n}{p} \|\boldsymbol{\eta}\|_2^2 + C_4\right) \\
&\leq C_5 \frac{n^2}{p^2} \left(\|\boldsymbol{\eta}\|_2^2 + \frac{p}{n}\right),
\end{aligned}$$

where we also use the fact $(a+b)^2 \leq 2(a^2 + b^2)$. Combining above results gives with probability at least $1 - \delta$,

$$\frac{(\mathbf{y}^T(\mathbf{X}\mathbf{X}^T)^{-1}\mathbf{X}\boldsymbol{\eta})^2}{\mathbf{y}^T(\mathbf{X}\mathbf{X}^T)^{-1}\mathbf{y}} \geq \|\boldsymbol{\eta}\|_2^2 \frac{\left((1 - \frac{n}{p})\|\boldsymbol{\eta}\|_2 - C_3\right)^2}{C_6(\frac{p}{n} + \|\boldsymbol{\eta}\|_2^2)}. \quad (23)$$

This completes the proof of the theorem.

D. PROOF OF LEMMAS 2, 3 AND 4

D.1. Proof of Lemma 2

The proof of Theorem 2 gives

$$\hat{\boldsymbol{\eta}} \cdot \boldsymbol{\eta} = \frac{s(\|\boldsymbol{\eta}\|_2^2 - t) + h^2 + h}{D},$$

for $D > 0$. Then (20) to (22) completes the proof.

D.2. Proof of Lemma 3

Recall

$$\mathbf{X}\mathbf{X}^T = \mathbf{Q}\mathbf{Q}^T + \|\boldsymbol{\eta}\|_2^2 \mathbf{y}\mathbf{y}^T + \mathbf{Q}\boldsymbol{\eta}\mathbf{y}^T + \left(\mathbf{Q}\boldsymbol{\eta}\mathbf{y}^T\right)^T = \mathbf{U} + \left[\|\boldsymbol{\eta}\|_2 \mathbf{y}, \mathbf{d}, \mathbf{y}\right] \begin{bmatrix} \|\boldsymbol{\eta}\|_2 \mathbf{y}^T \\ \mathbf{y}^T \\ \mathbf{d}^T \end{bmatrix}.$$

Thus, by Woodbury identity [HJ12], $(\mathbf{X}\mathbf{X}^T)^{-1}$ can be expressed as:

$$\mathbf{U}^{-1} - \mathbf{U}^{-1} \left[\|\boldsymbol{\eta}\|_2 \mathbf{y}, \mathbf{d}, \mathbf{y}\right] \left[\mathbf{I} + \begin{bmatrix} \|\boldsymbol{\eta}\|_2 \mathbf{y}^T \\ \mathbf{y}^T \\ \mathbf{d}^T \end{bmatrix}\right] \mathbf{U}^{-1} \left[\|\boldsymbol{\eta}\|_2 \mathbf{y}, \mathbf{d}, \mathbf{y}\right]^{-1} \begin{bmatrix} \|\boldsymbol{\eta}\|_2 \mathbf{y}^T \\ \mathbf{y}^T \\ \mathbf{d}^T \end{bmatrix} \mathbf{U}^{-1}. \quad (24)$$

We first compute the inverse of the 3×3 matrix $\mathbf{A} := \left[\mathbf{I} + \begin{bmatrix} \|\boldsymbol{\eta}\|_2 \mathbf{y}^T \\ \mathbf{y}^T \\ \mathbf{d}^T \end{bmatrix}\right] \mathbf{U}^{-1} \left[\|\boldsymbol{\eta}\|_2 \mathbf{y}, \mathbf{d}, \mathbf{y}\right]$. By our definitions of s, h and t in Section A,

$$\mathbf{A} = \begin{bmatrix} 1 + \|\boldsymbol{\eta}\|_2^2 s & \|\boldsymbol{\eta}\|_2 h & \|\boldsymbol{\eta}\|_2 s \\ \|\boldsymbol{\eta}\|_2 s & 1 + h & s \\ \|\boldsymbol{\eta}\|_2 h & t & 1 + h \end{bmatrix}$$

Standard matrix calculations give

$$\mathbf{A}^{-1} = \frac{1}{\det(\mathbf{A})} \text{adj}(\mathbf{A}),$$

where $\det(\mathbf{A})$ is the determinant of \mathbf{A} and $\text{adj}(\mathbf{A})$ is the adjoint of \mathbf{A} . It can be checked that:

$$\det(\mathbf{A}) = D = s(\|\boldsymbol{\eta}\|_2^2 - t) + (h+1)^2,$$

and

$$\text{adj}(\mathbf{A}) = \begin{bmatrix} (h+1)^2 - st & \|\boldsymbol{\eta}\|_2(st - h - h^2) & -\|\boldsymbol{\eta}\|_2s \\ -\|\boldsymbol{\eta}\|_2s & h+1 + \|\boldsymbol{\eta}\|_2^2s & -s \\ \|\boldsymbol{\eta}\|_2(st - h - h^2) & \|\boldsymbol{\eta}\|_2^2h^2 - t(1 + \|\boldsymbol{\eta}\|_2^2s) & h+1 + \|\boldsymbol{\eta}\|_2^2s \end{bmatrix}.$$

Combining the above gives

$$\begin{aligned} \mathbf{y}^T(\mathbf{X}\mathbf{X}^T)^{-1} &= \mathbf{y}^T\mathbf{U}^{-1} - \left[\|\boldsymbol{\eta}\|_2s, h, s\right]\mathbf{A}^{-1} \begin{bmatrix} \|\boldsymbol{\eta}\|_2\mathbf{y}^T \\ \mathbf{y}^T \\ \mathbf{d}^T \end{bmatrix} \mathbf{U}^{-1} \\ &= \mathbf{y}^T\mathbf{U}^{-1} - \frac{1}{D} \left[\|\boldsymbol{\eta}\|_2s, h^2 + h - st, s\right] \begin{bmatrix} \|\boldsymbol{\eta}\|_2\mathbf{y}^T \\ \mathbf{y}^T \\ \mathbf{d}^T \end{bmatrix} \mathbf{U}^{-1}. \end{aligned}$$

This completes the proof of the lemma.

D.3. Proof of Lemma 4

To prove Lemma 4, we need to bound the eigenvalues of \mathbf{U} . The following Lemma is a direct result of [BLLT20, Lemma 10] with $k = 0$ and $\Sigma = \mathbf{I}$.

Lemma 6. *Assume $p > bn$, for some $b > 1$. Suppose that $\delta < 1$ with $\log(1/\delta) < n/c$ for some $c > 1$. There is a constant $C_1 > 1$ such that with probability at least $1 - \delta$, the largest and smallest eigenvalues of \mathbf{U} satisfy:*

$$\frac{1}{C_1}p \leq \lambda_n(\mathbf{U}) \leq \lambda_1(\mathbf{U}) \leq C_1p. \quad (25)$$

Now we are ready to prove Lemma 4.

For $s = \mathbf{y}^T\mathbf{U}^{-1}\mathbf{y}$, from (25) and $\|\mathbf{y}\|_2^2 = n$, Cauchy-Schwarz inequality gives:

$$s \leq \|\mathbf{y}\|_2^2\lambda_1(\mathbf{U}^{-1}) \leq n\frac{1}{\lambda_n(\mathbf{U})} \leq C_1\frac{n}{p}.$$

The lower bound can be derived in a similar way and is omitted for brevity.

When bounding $t = \mathbf{d}^T\mathbf{U}^{-1}\mathbf{d}$ and $h = \mathbf{y}^T\mathbf{U}^{-1}\mathbf{d}$, recall $\mathbf{d} = \mathbf{Q}\boldsymbol{\eta}$. The singular value decomposition (SVD) of \mathbf{Q} is

$$\mathbf{Q} = \mathbf{U}'\boldsymbol{\Lambda}'^{\frac{1}{2}}\mathbf{V}'^T,$$

where \mathbf{U}' and $\boldsymbol{\Lambda}'^{\frac{1}{2}}$ are $n \times n$ matrices, \mathbf{V}' is a $p \times n$ matrix. By the SVD above, $\mathbf{U} = \mathbf{Q}\mathbf{Q}^T = \mathbf{U}'\boldsymbol{\Lambda}'^{\frac{1}{2}}\mathbf{U}'^T$, $\mathbf{d} = \mathbf{U}'\boldsymbol{\Lambda}'^{\frac{1}{2}}\mathbf{V}'^T\boldsymbol{\eta}$. $\mathbf{U}'\boldsymbol{\Lambda}'^{\frac{1}{2}}\mathbf{U}'^T$ gives the eigendecomposition of \mathbf{U} . By the definition of t and h ,

$$t = \boldsymbol{\eta}^T\mathbf{V}'\mathbf{V}'^T\boldsymbol{\eta}, \quad h = \mathbf{y}^T\mathbf{U}'\boldsymbol{\Lambda}'^{-\frac{1}{2}}\mathbf{V}'^T\boldsymbol{\eta}.$$

For t , by rotational invariant of \mathbf{Q} , \mathbf{V}'^T is right-rotationally invariant, meaning that the rows of \mathbf{V}'^T are uniformly orthogonal on the unit sphere. Then [Ver18, Lemma 5.3.2] gives with probability at least $1 - \delta$,

$$C_1\frac{n}{p}\|\boldsymbol{\eta}\|_2^2 \leq t \leq C_2\frac{n}{p}\|\boldsymbol{\eta}\|_2^2. \quad (26)$$

For h , by Cauchy-Schwarz inequality,

$$-\|\mathbf{y}^T\mathbf{U}'\|_2\|\boldsymbol{\Lambda}'^{-\frac{1}{2}}\|_2\|\mathbf{V}'^T\boldsymbol{\eta}\|_2 \leq h \leq \|\mathbf{y}^T\mathbf{U}'\|_2\|\boldsymbol{\Lambda}'^{-\frac{1}{2}}\|_2\|\mathbf{V}'^T\boldsymbol{\eta}\|_2.$$

Thus, (25), (26) and the fact that \mathbf{U}' is orthogonal give the advertised bounds.

The derivation of the bound for f_i is similar to that of h , except for \mathbf{y} in h is replaced by \mathbf{e}_i in f_i , so the norm of $\|\mathbf{y}\|_2 = \sqrt{n}$ is replaced by $\|\mathbf{e}_i\|_2 = 1$. The proof is omitted for brevity. This completes the proof of the lemma.